The Potential of Using the Ion-Current Signal for Optimizing Engine Stability - Comparisons of Lean and EGR (Stoichiometric) Operation

Einewall, Patrik; Tunestål, Per; Johansson, Bengt

Published in:
SAE Special Publications

DOI:
10.4271/2003-01-0717

2003

2003-01-0717

The Potential of Using the Ion-Current Signal for Optimizing Engine Stability — Comparisons of Lean and EGR (Stoichiometric) Operation

Patrik Einewall, Per Tunestål and Bengt Johansson
Lund Institute of Technology

ABSTRACT

Ion current measurements can give information useful for controlling the combustion stability in a multi-cylinder engine. Operation near the dilution limit (air or EGR) can be achieved and it can be optimized individually for the cylinders, resulting in a system with better engine stability for highly diluted mixtures. This method will also compensate for engine wear, e.g. changes in volumetric efficiency and fuel injector characteristics. Especially in a port injected engine, changes in fuel injector characteristics can lead to increased emissions and deteriorated engine performance when operating with a closed-loop lambda control system. One problem using the ion-current signal to control engine stability near the lean limit is the weak signal resulting in low signal to noise ratio. Measurements presented in this paper were made on a turbocharged 9.6 liter six cylinder natural gas engine with port injection. Each cylinder was individually controlled by a cylinder control module (CCM). A high turbulence combustion chamber was used to be able to operate with highly diluted mixtures. Comparisons between lean and EGR (stoichiometric) operation were made to investigate the potential of using the ion-current signal to control engine stability (cylinder to cylinder and cycle to cycle variations). A much stronger ion-current signal was found with EGR compared to lean operation, for the same load and comparable emissions.

INTRODUCTION

One way to improve fuel economy is to operate the engine with diluted mixtures, addition of extra air (lean operation) and/or exhaust gas recalculation. A diluted mixture lowers the combustion temperature, resulting in less heat losses and emissions of nitric oxides (NO_x). The pump losses at part load are also reduced with lean and /or EGR operation. Many truck size natural gas engines are diesel engines converted to natural gas operation. This often limits the exhaust temperature, so the engines can not be spark ignited (SI) with stoichiometric mixtures without dilution.

The way to operate an engine is a tradeoff between good fuel economy and low emissions of hydrocarbons, HC, carbon monoxide, CO, soot and NO_x. A very good fuel economy can be achieved with lean operation, such as diesel-operation and HCCI-operation, Homogenous Charge Compression Ignition. Stoichiometric SI-operation with a tree way catalyst results in very low emissions (not carbon dioxide, CO_2 included). One way to get better fuel economy (higher efficiency) than pure stoichiometric SI-operation, and lower emissions than lean operation is by addition of EGR to a stoichiometric mixture, and use a three way catalyst.

The difficulty of mixing air and natural gas can be a problem in a lean burn single point fuel-injected gas engine. A well mixed mixture (injecting upstream the turbo-compressor) may lead to reduced efficiency and long response time, between injecting fuel and measuring the lambda value in the exhaust. This leads to a disadvantage in transient behavior. If the engine is operated at lambda 1.1 at idle and 1.6 at full load, a transient from idle to full load results in full load operation at lambda 1.1 during a short time, thus forming much NO_x. Injecting fuel closer to the cylinders may lead to a stratified mixture, resulting in different lambda values between the cylinders and higher cycle to cycle and cylinder to cylinder variations [1]. One way to control the amount of fuel entering each cylinder is to have port-injection and in some way measure the mixture composition or combustion in all cylinders. This can be achieved by e.g. multiple lambda probes, cylinder-pressure measurements or ion-current measurements.

Controlling the engine with information from the ion-current may be a problem at lean operation, because of the weak signal at those conditions. As will be seen in this paper, dilution with EGR at stoichiometric operation results in a much stronger ion-current signal, which could be used to control and balance each cylinder.

The aim of this paper is to compare lean operation with EGR (stoichiometric) operation and study emissions (raw emissions), heat release and ion-current signal.

EXPERIMENTAL APPARATUS

THE ENGINE

The Engine (TG103/G10A) was originally developed for diesel operation and redesigned by Volvo for natural gas operation, see Table 1 for specifications. The fuel is port-injected and the engine is equipped with a cooled EGR system, Figure 2.

Table 1. Engine Specifications

Displaced volume/cyl.	1600 cm^3
Compression ratio	11.8:1
Rated power	184 kW (at 2000 rpm)
Maximum brake torque	1150 Nm (at 1150 rpm)
Bore	120.65 mm
Stroke	140 mm
Ignition sequence	1-5-3-6-2-4

NATURAL-GAS PORT-INJECTION SYSTEM

The street version of the vehicles using this engine has single point injection using four injectors at the fuel injector assembly. The gas pressure is approximately 10 bar (a). The test bench engine is supplied with natural gas at 4.6 bar (a), so the port injection system is equipped with 12 injectors (2 per cylinder) to be able to cover the whole load range, Figure 1. This also makes it possible to operate the engine with two different gaseous fuels simultaneously. An extension of the intake ports prevents cross breathing of natural gas between cylinders at high loads. The total volume of each inlet port is slightly larger than half the displacement volume per cylinder.

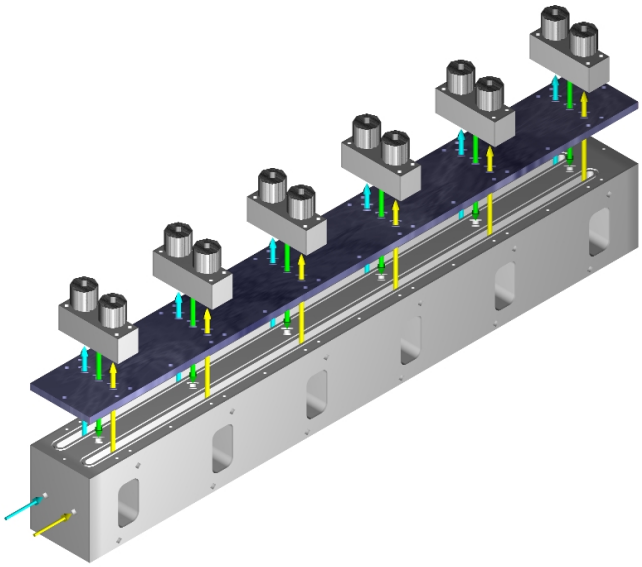

Figure 1. The port injection system.

Fuel injection timing

Mixing air and natural gas may be a problem using port injection [2]. Injection timing was selected to be centered around TDC gas-exchange at low to medium injection duration, and early enough to finish injection 30 degrees before inlet valve closing (IVC at 230 degrees ATDC) for long injection duration. This strategy ensures sufficient air-flow past the inlet valve for mixing of air and natural gas. If the fuel is injected after IVC the next cycle will receive a stratified charge due to poor mixing.

ENGINE CONTROL SYSTEM

A PC controls each cylinder individually via six cylinder control modules (CCM) from MECEL. A crank angle encoder (1800 pulses per revolution) is connected to the CCM's, and provides speed and crank angle information. The CCM's compute the ion-current integral for each cylinder and cycle and sends the information to the PC. The raw ion-current signal is also accessible. The following parameters can be set from the PC:

- Fuel injection (timing and duration) for each cylinder
- Ignition timing for each cylinder
- Window for computing ion-current integral
- Lambda value
- Wastegate control
- Engine dynamometer speed
- Amount of EGR

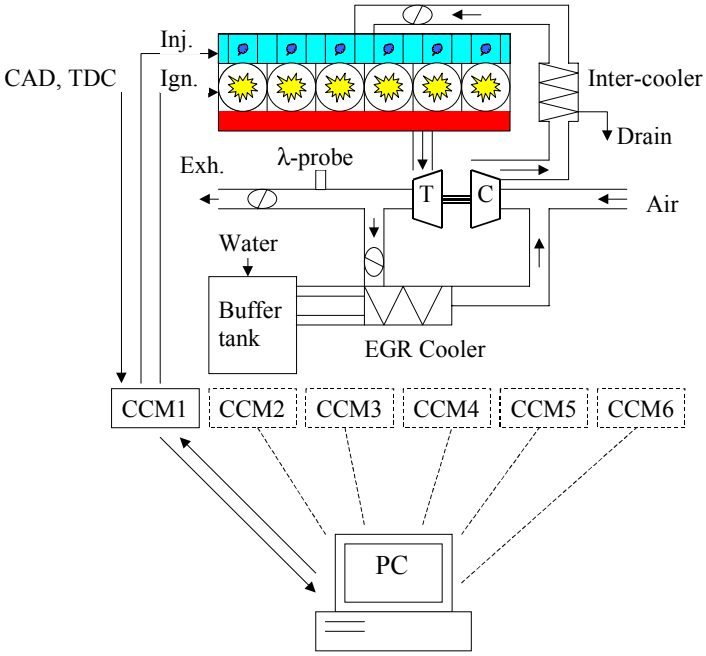

Figure 2. The Engine.

EGR SYSTEM

A long root cooled EGR system is used. An exhaust-gas heat exchanger is used to cool the EGR. Water from a buffer tank, with water maintained at a constant temperature, is circulated through the heat exchanger to control the EGR temperature (approximately 60 ° C). Both hot and cold water is connected to the buffer tank. A throttle on the inlet of the exhaust-gas side of the EGR cooler controls the amount of EGR delivered to the engine. A throttle at the end of the exhaust pipe is used to further increase the amount of EGR (if the EGR-throttle is fully open and not enough EGR is delivered). The amount of EGR is computed according to:

$$\%EGR = \frac{CO_2 inlet}{CO_2 exhaust} * 100 \quad \%\text{-vol}$$

Where $CO_2 inlet$ is compensated for the injected fuel.

SUPPLY SYSTEMS

Pressure

Each cylinder head is equipped with a piezo electric pressure transducer, Kistler 7061B. The signal from the charge amplifier, Kistler 5017A, is processed by two parallel Datel PCI-416 boards in a PC for on line pressure measurements. The cylinder pressures are measured 5 times per crank angle degree (CAD) using an external clock from a Leine & Linde crank-angle encoder. The pressures are used for heat-release calculations, the program is described in [3]. Pressures are also measured in the inlet manifold (before and after the throttle) and in the exhaust pipe, before the exhaust throttle.

Emissions

Emissions are measured after the turbocharger. The emissions are measured by a Pierburg AMA 2000 emission system consisting of; a Heated Flame Ionization Detector (HFID/FID) for hydrocarbons, a Heated Chemiluminescence Detector (HCLD/CLD) for nitric oxides and a Paramagnetic Detector (PMD) for oxygen (O_2). The HC emissions are presented as methane equivalent (C1) in the figures. Four Non Dispersive Infra-red Detectors (NDIR) measures carbon monoxide (CO high and low) and carbon dioxide (in the exhaust and in air/EGR mixture).

In addition to lambda calculations, a lean lambda probe (ETAS) is installed in the exhaust pipe, after the turbocharger.

Temperatures

Probes for temperature measurements are located between the exhaust valve and exhaust manifold on all six cylinder heads, for cylinder individual measurements. Temperatures on the EGR system are measured on the hot and the cold side, both for exhaust gas and cooling water. The temperature probes (Pentronic) on the hot side are shielded. Supervising temperatures are measured in the inlet manifold, cooling water and engine oil.

Flows

The mass flow of natural gas is measured with a Bronkhorst F106A-HC.

Torque

The engine is connected to a Schenk U2-30G water brake, controlled by the engine control system. The torque is measured with a load cell, Nobel Elektronik KRG-4.

All data, except in-cylinder pressure, is collected by a HP 34970A Data Acquisition/Switch unit.

COMBUSTION CHAMBER

A fast burning combustion chamber, having high turbulence, is used to enable operation with highly diluted mixtures, see Figure 3. One drawback with a fast burning combustion chamber is that the exhaust gases are colder. The turbocharger is optimized for the original slow burning combustion chamber called Turbine, see Figure 3. Even if a fast combustion chamber is more tolerant for diluted mixtures, the cold exhaust gases result in too low boost pressure at lean conditions. Figure 4 show pressure traces for Quartette and Turbine at 950 Nm, lambda 1.4 and ignition timing 10 CAD before top dead center (BTDC).

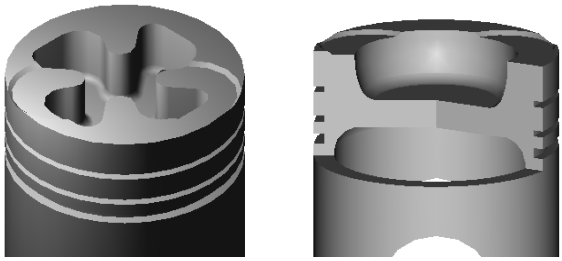

Figure 3. Quartette (left) and Turbine (right) combustion chambers.

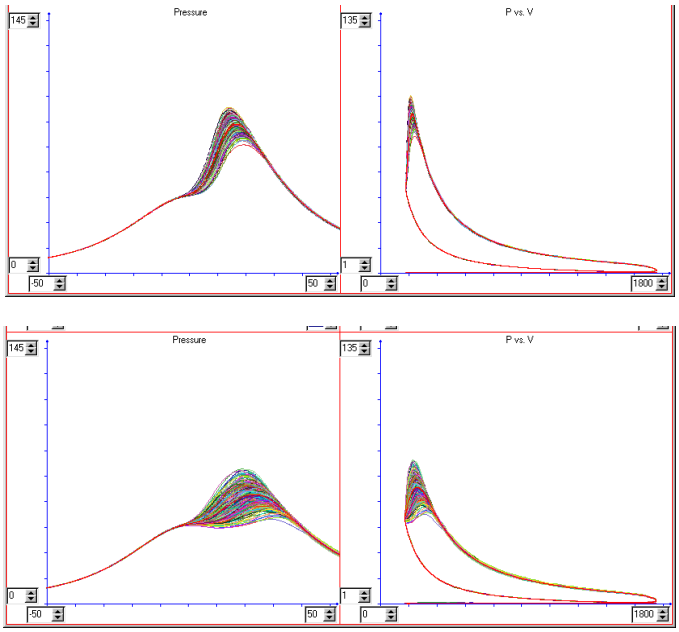

Figure 4. Pressure traces (left – pressure v.s. CAD, right - pressure v.s. volume) for Quartette (top) and Turbine (bottom) at 950 Nm, lambda 1.4 and ignition timing 10 CAD BTDC.

ION CURRENT MEASUREMENTS

The principle of ion current measurements is to apply a constant voltage (~100 volt) over the spark gap after ignition. When the gas in the gap becomes conductive due to ionization of the charge a current flows through the spark gap. This current is sampled by the CCM's. It is not fully understood all factors influencing the ion-current signal in SI engines. There are often two current peaks, the first is believed to be the result of the small flame kernel passing the spark electrodes, and the second appearing close to the maximum cylinder pressure (some CAD before in this study), see Figure 18. One model for the second ion-current peak was presented by Saitzkoff et al. [4], where the main factor the peak was thermal ionization of NO. Another model was presented by S. Yoshiyma et al. [5], where the flame-front contact with the cylinder wall/piston crown contributes to the second ion-current peak.

EXPERIMENT

The tests are conducted at 1100 rpm and 950 Nm with various ignition angles, amounts of EGR and air/fuel ratios. To keep the same load for the different cases, some tests are conducted with wide open throttle (not enough boost to get more than 950 Nm) and some tests are throttled, see Table 2 for test matrix. It was not possible to operate leaner than lambda 1.55, the boost was not enough to get 950 Nm. This was due to the fast combustion chamber, resulting in reduced exhaust temperature compared to the original combustion chamber.

Table 2. Test matrix. Rows: Mixture (EGR % -top, or lambda -bottom). Columns: Ignition CAD BTDC.

	5	10	15	20	25	30	35
25				X	X/O	X	X
22.5		X	X	X	X/O	X	
20		X	X	X/O	X		
17.5	X	X	X/O	X			
15	X	X	X/O				
12.5	X	X	X/O				
10	X	X/O					
1.55	X	X	X/O				
1.50	X	X	X/O	X			
1.47	X	X	X/O	X			
	Misfire						
	Insufficient boost pressure						
	Knock						
X: Could be operated, O: MBT ignition timing							

RESULTS

The operating points according to Table 2 are first evaluated in terms of emissions, performance and efficiency in order to find out whether stoichiometric operation with EGR is a viable alternative to lean operation. Subsequently the ion-current characteristics for EGR and lean operation are compared. Most of the plots include both various amounts of EGR and air-fuel ratios (presented as lambda) at MBT ignition timing. MBT ignition timing is selected as the timing resulting in the lowest brake specific fuel consumption, bsfc. Exact MBT timing may deviate from the presented ignition angles, since the tests are conducted in steps of five CAD.

EMISSIONS

Emissions measured after the turbocharger are presented in terms of brake specific emissions (g/kWh) and in some cases also in terms of raw concentration levels. Mass flow through the engine is lower with EGR (for amounts presented in this paper) than lean operation, so specific emissions are favored when operating with EGR.

Figure 5 shows HC emissions vs. dilution levels of EGR and air. HC concentrations are generally higher with EGR than with excess air, but he specific emissions are lower with EGR due to less mass flow. Air-fuel ratio has a stronger influence on HC emissions than the amount of EGR, leaner operation increases HC emissions.

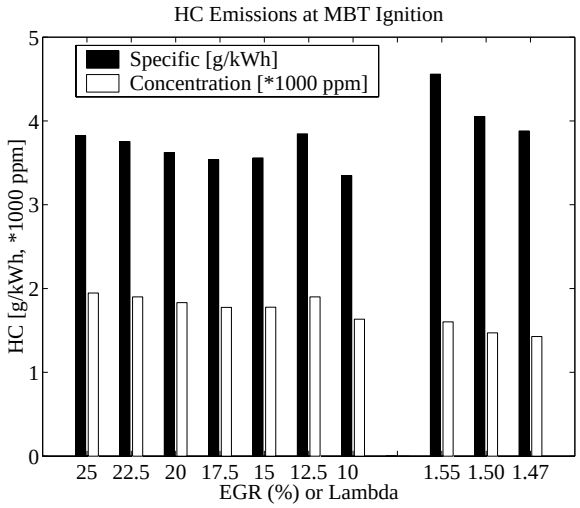

Figure 5. HC emissions in g/kWh and concentration (*1000 ppm) at MBT ignition.

NO_x emissions as shown in Figure 6 are reduced with increasing EGR and excess air, as expected. Also here the lower mass flow with EGR results in less specific NO_x emissions compared to lean operation.

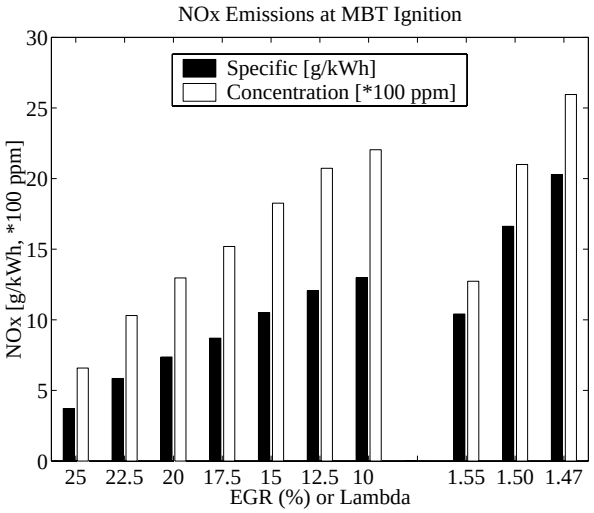

Figure 6. NO_x emissions in g/kWh and concentration (*100 ppm) at MBT ignition.

In Figure 7 the influence of ignition timing on NO_x emissions can be seen for 17.5% EGR compared to lambda 1.50. Advanced ignition timing increases the emissions for both EGR and lean operation. EGR is less sensitive than lean operation with respect of ignition timing. With EGR the emissions increases from approximately 5 to 10 g/kWh, with excess air the increase is from 5 to 25 g/kWh, when ignition timing goes from 5 to 20 CAD BTDC. This makes it possible to operate close to MBT ignition with EGR without increasing NO_x emissions. At lean operation a retarded ignition angle is often used to lower the NO_x emissions. This strategy will lead to deteriorated performance and efficiency.

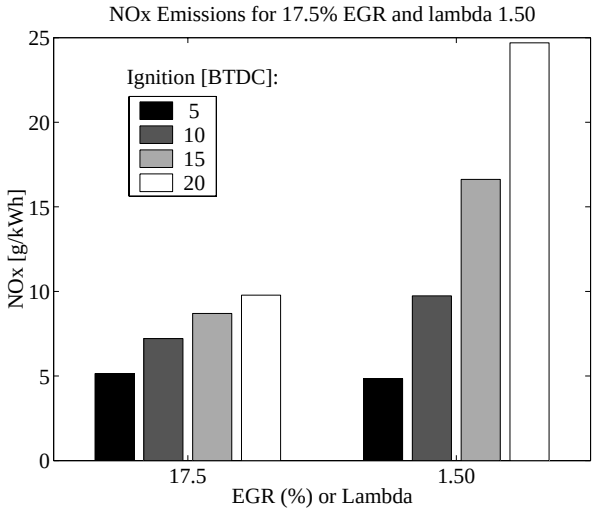

Figure 7. Specific NO_x emissions with respect to ignition timing for 17.5% EGR and lambda 1.50.

The CO emissions are much higher with EGR than lean burn, Figure 8. Since the EGR tests are at stoichiometric conditions the CO emissions are expected to be higher. The trend with EGR is that the specific emissions decreases with increased amount of EGR. For lean operation the specific emissions increases when excess air is increased. CO concentrations are not much affected by various amounts of EGR [6].

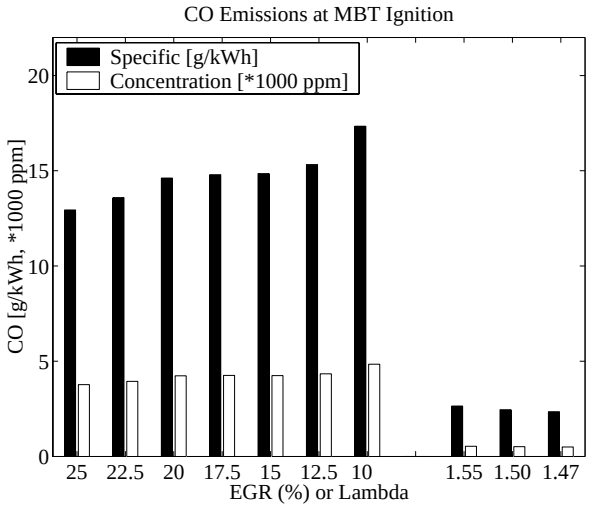

Figure 8. CO emissions in g/kWh and concentration (*1000 ppm) at MBT ignition timing.

COMBUSTION

Cycle to cycle variations (as COV_{IMEP}) and heat release are shown in the following figures.

Coefficients of Variation (COV) for Indicated Mean Effective Pressure (IMEP) are shown in Figure 9. Operating with both EGR and excess air give quite low cycle to cycle variations (less then 5% is considered to be low [6]). It was not expected to see that the cycle to cycle variations decreases with increasing amount of EGR, this will be discussed later. The trend for lean operation is more expected, COV increases with lambda.

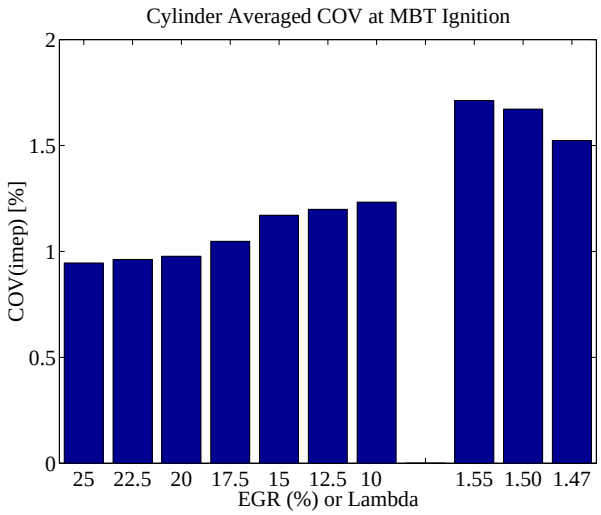

Figure 9. Cylinder averaged COV(IMEP) at MBT ignition.

The flame development period (0-5% burned) and main combustion (10-90% burned) can be seen in Figure 10. Both early and main combustion increases when EGR or excess air increases. The main combustion duration is similar for both EGR and lean operation. The early combustion period increases strongly at high amounts of EGR. It is known that EGR has a stronger influence than excess air on laminar flame speed [6]. This can explain the strong influence on the early combustion with high EGR dilution. The rather fast main combustion can be explained by the high turbulence peak at TDC. Figure 11 shows the turbulence measured at the spark plug position using Laser Doppler Velocimetry, LDV. Even if the laminar flame speed is much reduced with EGR, the high turbulence close to TDC results in a fast main combustion.

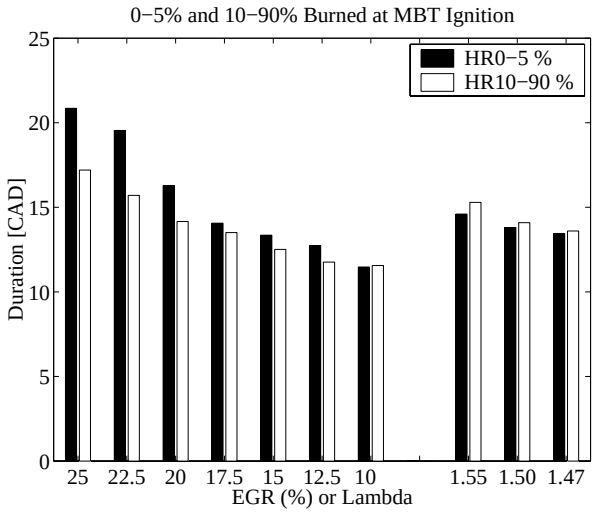

Figure 10. Flame development period (0-5% burned) and main combustion (10-90% burned) at MBT ignition.

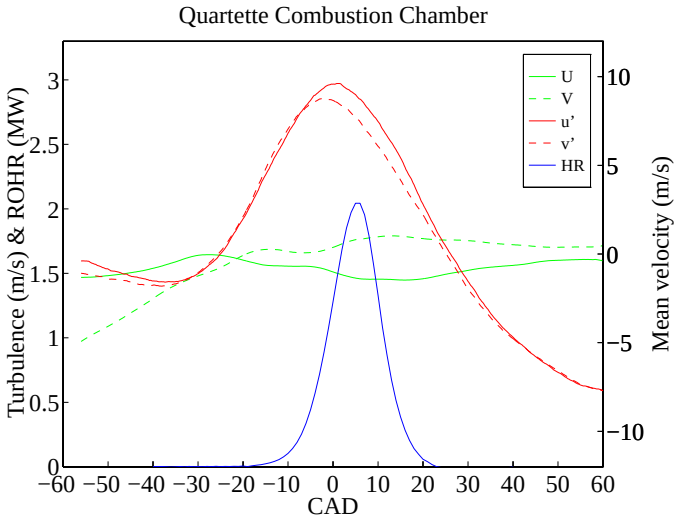

Figure 11: Mean velocity (almost constant) and turbulence data in two directions, 5 mm below the spark plug. Heat release rate at the bottom of the figure. The engine was operated at 1200 RPM, 1 bar inlet pressure and λ=1.5.

EFFICIENCY

Figure 12 shows the contribution from various effects on brake efficiency. Highest brake efficiency is obtained at lean operation. Brake efficiency increases with increasing amount of EGR. Most of the difference in brake efficiency between EGR and lean operation can be explained by a lower combustion efficiency operating with EGR. The high CO emissions are the main reason for the decreased combustion efficiency. Also gas-exchange efficiency ($IMEP_{net}/IMEP_{gross}$) is lower with EGR. The main reason for this is that the exhaust gases

are throttled in order to deliver enough EGR, resulting in increased pump losses. With low amounts of EGR the engine is not operated at wide open throttle (WOT), resulting in pump losses. Even when these losses are considered the resulting efficiency is higher at lean conditions. The mechanical efficiency is assumed to be equal for both cases, since the operating points are similar in terms of cylinder pressure. A zero dimensional cycle simulation [7] was used to study the effects of mixture composition. The simulated efficiencies shows a difference between 25% EGR and λ 1.55, which can explain some of the remaining difference. One factor is that the specific heat (C_p) is higher with EGR, The bulk gases absorbs more heat. More fuel is then needed to get the same work from the engine. One other factor is that the maximum cylinder temperature with EGR is higher than at λ 1.55, leading to higher heat losses.

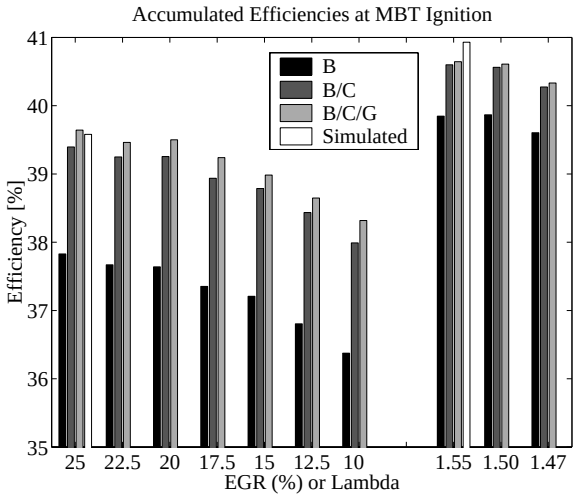

Figure 12. Efficiency compensated for various effects. B: brake efficiency, B/C: efficiency compensated for combustion efficiency, B/C/G: efficiency compensated for combustion efficiency and pump losses, Simulated: zero dimensional cycle simulation.

ION-CURRENT MEASUREMENTS

Now that the engine behavior with stoichiometric-EGR and lean operation has been compared, it remains to compare the ion-current characteristics. This section discusses the influence of EGR and excess air on the ion-current signal, averaged over 300 cycles. All measurements of the raw ion-current trace refer to cylinder 1. The ion-current integral is however available for all six cylinders.

The amplitude of the first peak decreases with increased dilution, both with EGR and excess air (Figure 13). The amplitude is much higher with EGR than at lean conditions. With 25% EGR the first peak appears so late in the cycle that the first and second peaks coincide. With 10% EGR the first peak appears so early that is disappears in the ignition noise.

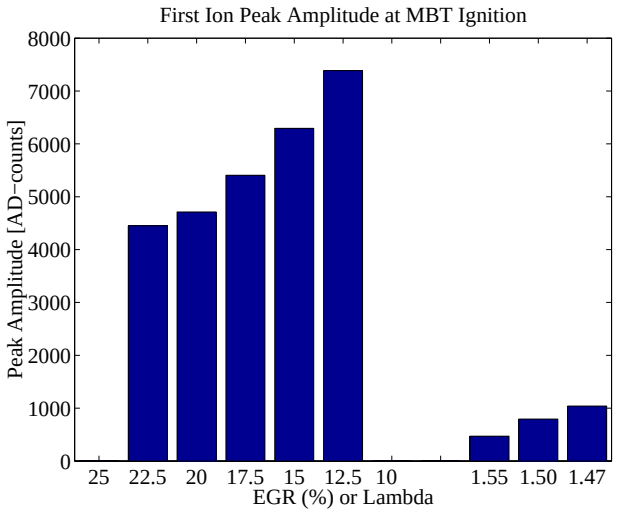

Figure 13. Ion-current first ion peak amplitude at MBT ignition.

There is no detectable second ion-current peak at very lean conditions with this ion-current measurement system. It is a known fact that the ion-current signal (especially the second peak) becomes very small at lean conditions [8], [9]. With EGR there is a strong signal, see Figure 14. This figure shows the second ion current peak amplitude for cylinder 1.

Figure 15 shows the ion-current integral (computed from 1 ms after ignition to 50 CAD ATDC) for all cylinders. There is a strong correlation between the amplitude and the integral (cylinder 1), even though the first peak is included in the integral. For EGR ratios between 10 and 17.5% a similar trend can be seen between cylinders, with the smallest integral at 17.5% and maximum at 12.5%. With higher amounts of EGR the ion-current integral differs between the cylinders, cylinder 1 has the largest integral at 25% EGR and cylinder 4 and 5 the lowest.

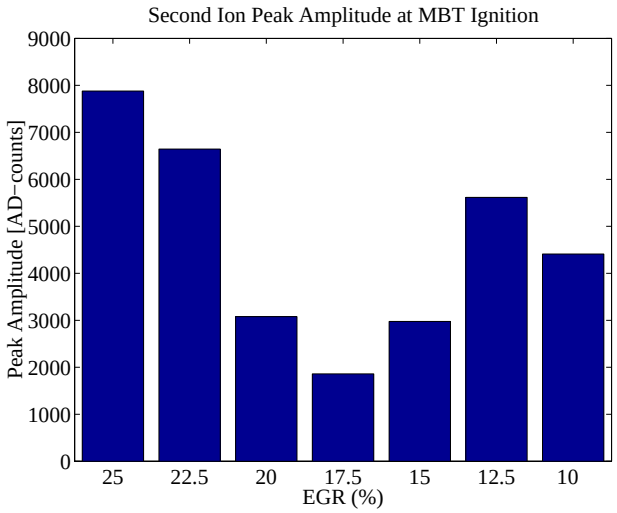

Figure 14. Ion-current second peak amplitude at MBT ignition (cylinder 1).

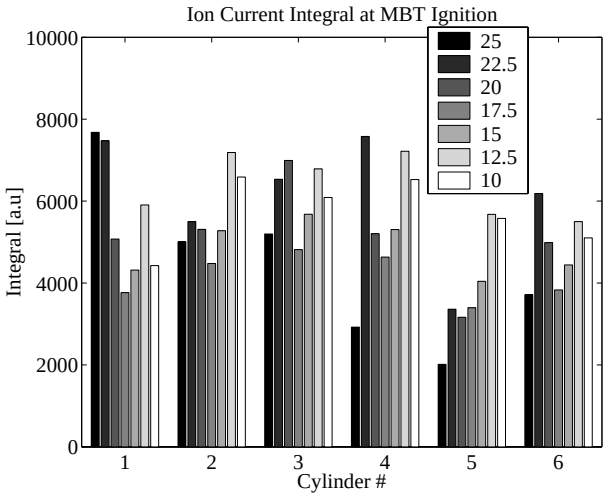

Figure 15. Ion current integral for all cylinders at MBT ignition. EGR values in legend.

There are several reports in the literature showing a strong correlation between the cylinder pressure and the ion-current [10] [11] [12]. Figure 16 shows the maximum cylinder pressure for all cylinders at MBT ignition and various amounts of EGR. For low EGR ratios 10% to 17.5% there is a strong correlation between ion-current integral and maximum pressure for all cylinders. With high dilution of EGR the maximum pressure differs some between the cylinders, but no correlation can be seen compared to ion-current integral.

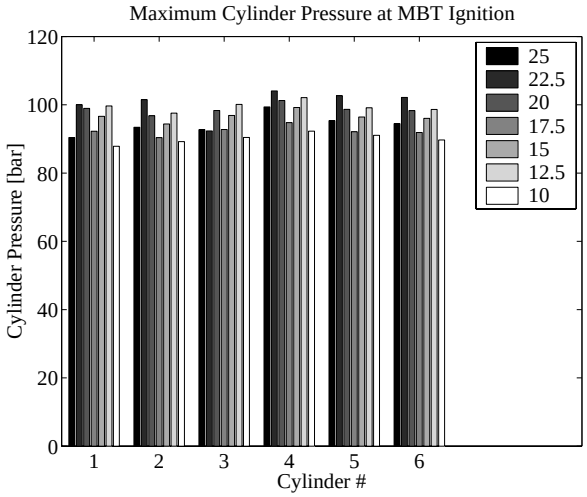

Figure 16. Maximum cylinder pressure for all cylinders at MBT ignition. EGR values in legend.

The raw ion-current signal was measured only in cylinder 1, and Figure 15 showed a large difference between the cylinders with high dilution of EGR. Therefore Figure 17 may not be representative for all cylinders. Figure 17 to Figure 20 shows ion-current signal and cylinder pressure (cylinder 1) for 25%, 17.5%, 10% EGR and λ 1.47, respectively. With 25% EGR (Figure 17) the first and second ion peaks coincide. With 17.5% EGR (Figure 18) the first ion peak is clearly separated from the second peak, and with 10% EGR (Figure 19) the first peak disappears in the noise from the ignition. At λ 1.47 the first peak is much smaller than with EGR and no second peak can be seen. At even leaner conditions the first peak decreases in amplitude.

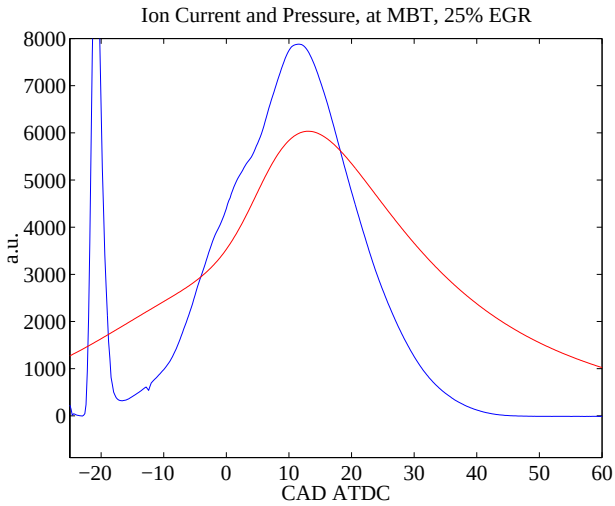

Figure 17. Averaged ion-current signal and cylinder pressure (cylinder 1) at MBT ignition and 25% EGR.

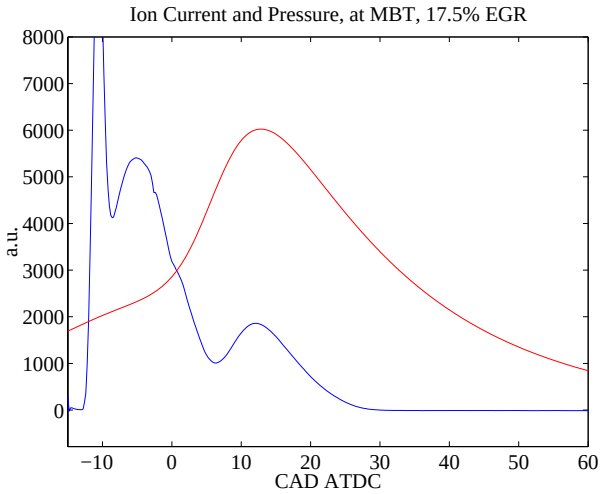

Figure 18. Averaged ion-current signal and cylinder pressure (cylinder 1) at MBT ignition and 17.5% EGR.

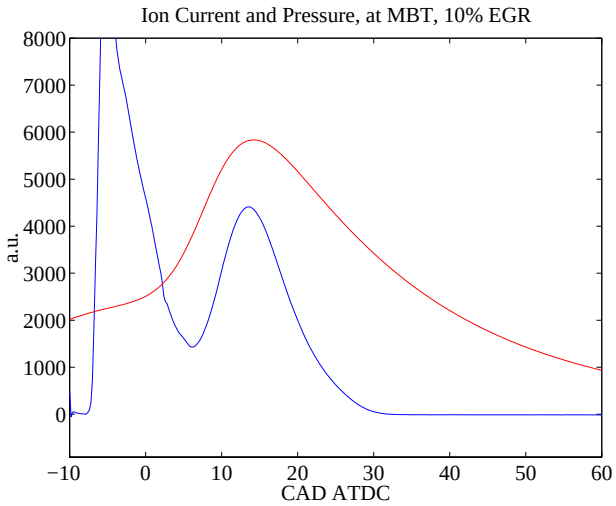

Figure 19. Averaged ion-current signal and cylinder pressure (cylinder 1) at MBT ignition and 10% EGR.

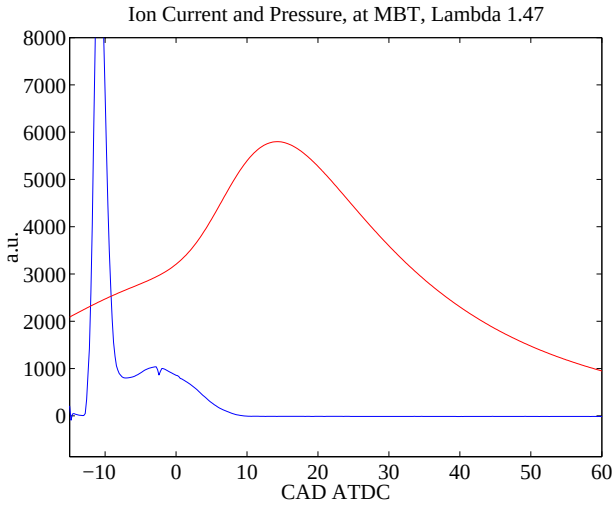

Figure 20. Averaged ion-current signal and cylinder pressure (cylinder 1) at MBT ignition and lambda1.47.

In Figure 21 volume percentage burned and mass percentage burned are plotted at the second ion-peak position, for various amounts of EGR (MBT ignition) for cylinder 1. The peak position correlates well with approximately 90%-vol burned for all EGR ratios. The correlation is not so strong for %-mass burned. The %-vol burned at the second peak position is also less dependant on ignition angle than %-mass burned (Figure 22). The heat release analysis renders %-mass burned (y_b). The relationship between y_b and x_b (%-vol) can be expressed as [6]:

$$x_b = \left[1 + \frac{\rho_u}{\rho_b}\left(\frac{1}{y_b} - 1\right)\right]^{-1}$$

Where ρ_u is the density of the unburned mixture and ρ_b is the burned gas density. y_b can then be expressed as:

$$y_b = \frac{4x_b}{1+3x_b}$$

Where ρ_u/ρ_b has been selected to 4 [6].

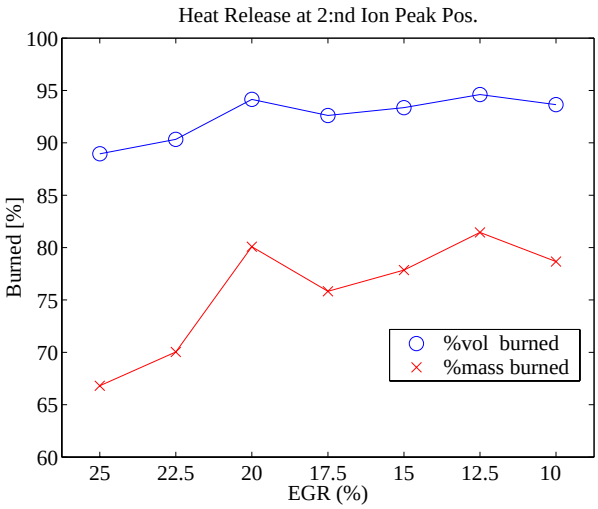

Figure 21. %-Vol burned and %-mass burned at the second ion-peak position, at MBT ignition and various amounts of EGR.

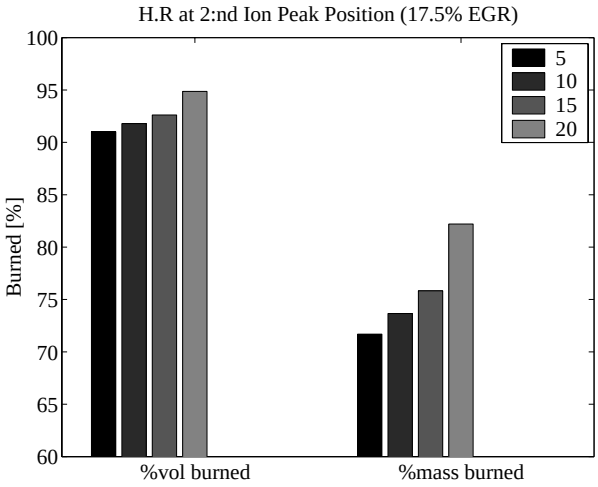

Figure 22. %-Vol burned and %-mass burned at the second ion-peak position with 17.5% EGR and various ignition angles (ignition angles in legend).

Previous studies have shown a strong correlation between the position of the second ion-current peak and the position of maximum cylinder pressure [10]. Figure 23 shows the crank angle between the second ion-peak position and maximum cylinder pressure, temperature respectively for a range of EGR ratios at MBT ignition. The crank angle between the second ion peak and cylinder pressure is approximately 2 CAD for all EGR ratios. The crank angle between the second ion peak

and maximum temperature increases with the amount of EGR. The temperatures are computed with a one-zone model [13].

Figure 24 shows that both cylinder pressure and temperature "pull" the second ion-current peak. At 10 CAD ignition angle, the maximum temperature appears late and the ion current peak is close to the maximum cylinder pressure. At 30 CAD ignition, maximum cylinder pressure and temperature are closer to each other, resulting in the ion-current peak moving further away from the maximum pressure position.

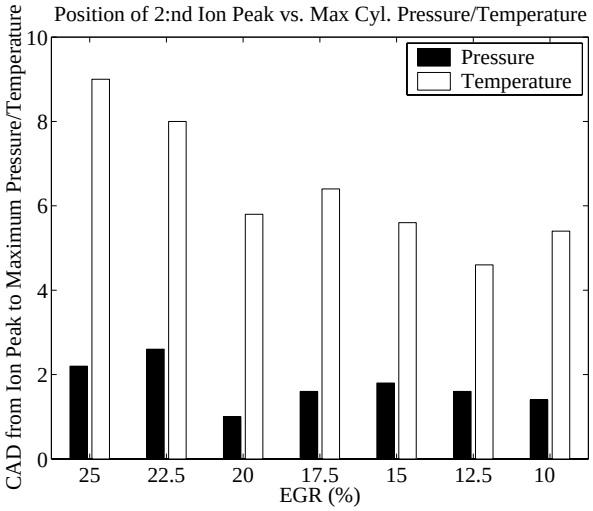

Figure 23. crank angle between the second ion peak and maximum pressure, temperature respectively. Various amounts of EGR at MBT ignition.

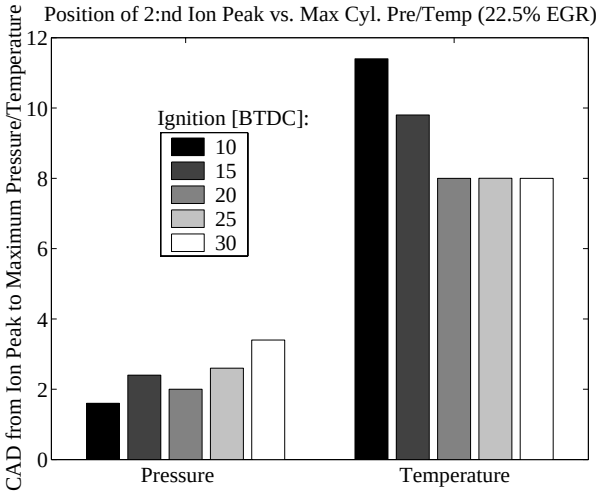

Figure 24. Crank angle between the second ion peak and maximum pressure, temperature respectively. With 22.5% EGR and various ignition angles.

Figure 25 shows the crank angle position in CAD ATDC for the maximum rate of heat release, RoHR, and cylinder pressure vs. the position for the second ion-current peak, for all EGR ratios and ignition angles. Linear regression was performed on the data:

$$y_p = k_p \theta_{ion} + m_p$$
$$y_{dQ} = k_{dQ} \theta_{ion} + m_{dQ}$$

where k_p=0.91, m_p=2.8, k_{dQ}=1.02 and m_{dQ}=-4.1.

The correlation coefficients are 0.994 and 0.995, respectively. The second ion-current peak thus appears approximately 4 CAD after the position for maximum RoHR for all EGR ratios and ignition angles. There is a linear relationship also for the maximum pressure, but the crank angle between pressure peak and ion-current peak varies ($k_p \neq 1$).

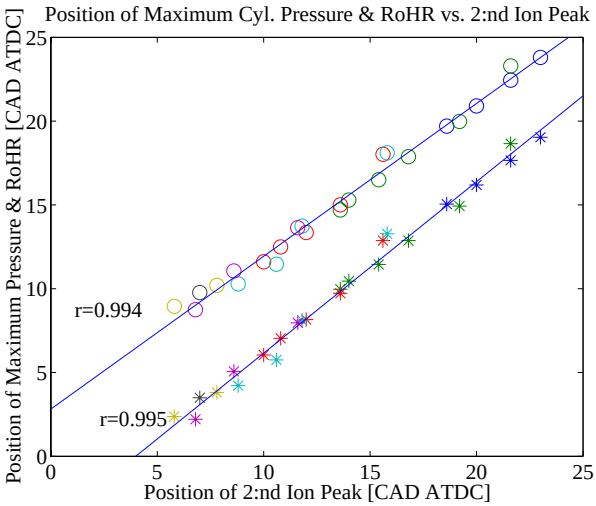

Figure 25. Crank angle position for maximum rate of heat release, RoHR (✳), and cylinder pressure (o) vs. position for the second ion-current peak, for all EGR ratios and ignition angles.

DISCUSSION

The unexpected trend for COV_{IMEP} (decreasing with increasing amounts of EGR) may be explained by a very thick (wrinkled) flame front with high amounts of EGR. A thick flame front (a large portion of the charge burns essentially at the same time, but slowly) should be less sensitive to local variations in air/fuel ratio, turbulence, bulk flow etc. This can be seen in HCCI combustion [14]. Some figures indicates that the flame front is thick.

- Figure 17 shows that the first ion-current peak and the second peak coincide. This indicates that the flame front passes the spark gap almost at the same time as it has contact with the piston crown (or cylinder wall), according to the model by S. Yoshiyma et al. [5].

- The decreasing trend in %-burned with increasing amounts of EGR (Figure 21) indicates that there are "pockets" of unburned mixture in the flame, a thick and wrinkled flame front.

CONCLUSIONS

Comparisons between EGR and lean operation show:

- Decreased specific HC emissions with EGR.
- Decreased specific NO_x emissions with high EGR ratios, as well as less sensitivity of NO_x emissions with respect to ignition timing.
- 5 times higher CO emissions with EGR.
- Decreasing cycle to cycle variations with increasing amount of EGR, possibly due to a thicker flame front with high amounts of EGR. Lower COV_{IMEP} with EGR than at lean operation.
- Strong influence of EGR on early combustion (slower). Comparable main combustion duration with EGR and lean operation. Fast main combustion due to high turbulence around TDC.
- Decreased brake efficiency with EGR. The main reason is the lower combustion efficiency.
- Strong ion-current signal with EGR (both first and second peak), very week at lean conditions because of no second peak.
- Strong correlation between the second ion-current peak position and volume percentage burned. Second peak appears in the range of 90% burned with the Quartette combustion geometry.
- Both maximum cylinder pressure and temperature positions affect the location of the second ion-current peak position.
- Very strong correlation between the position for maximum heat release and position of the second ion-current peak. There is a nearly constant crank angle delay of 4 CAD between the maximum RoHR and the second ion-current peak, for all EGR ratios and ignition angles.

ACKNOWLEDGMENTS

We would like to thank Swedish Gas Center, Volvo Truck Company, Scania, MECEL, Caterpillar and Swedish National Energy Administration for their support of the presented work.

REFERENCES

1. P. Einewall and B. Johansson:
"Cylinder to Cylinder and Cycle to Cycle Variations in a Six Cylinder Lean Burn Natural Gas Engine", SAE Spring Fuels and Lubricants Meeting, 2000.
2. P.V. Puzinauskas, B. D. Willson, K. H. Evans:
"Optimization of Natural Gas Combustion in Spark-Ignited Engines Through Manipulation of Intake-Flow Configuration", SAE paper 2000-01-1948
3. B. Johansson:
"On Cycle to Cycle Variations in Spark Ignition Engines", Doctoral Thesis, Lund Institute of Technology, 1995.
4. A. Saitzkoff, R. Reinmann, T. Berglind, M. Glavmo:
"An ionization equilibrium analysis of the spark plug as an ionization sensor", SAE paper 960337 (1996).
5. S. Yoshiyama, E. Tomita, Y. Hamamoto:
"Fundamental Study on Combustion Diagnostics Using a Spark Plug as Ion Probe", SAE paper 2000-01-2828.
6. J. B. Heywood:
"Internal Combustion Engine Fundamentals"
ISBN 0-07 100499-8.
7. O. Erlandsson:
"Development of an Engine System Simulation Software Package – ESIM"
ISRN LUTMDN/TMVK – 7043 Lund Institute of Technology report, 2000.
8. R. Reinmann, A. Saitzkoff, F. Mauss:
"Local Air-Fuel Ratio Measurements Using the Spark Plug as an Ionizatin Sensor", SAE paper 970856 (1997).
9. M. Hellring, T. Munther, T. Rognvaldsson, N. Wickstrom, C. Carlsson, M. Larsson, J. Nytomt:
"Robust AFR Estimation Using the Ion Current and Neural Networks", SAE paper 1999-01-1161.
10. A. Saitzkoff, R. Reinmann, F. Mauss:
"In-Cylinder Pressure Measurements Using the Spark Plug as an Ionization Sensor", SAE paper 970857 (1997).
11. Y. Ohashi, W. Fukui, F. Tanabe, A. Ueda:
"The Application of Ionic Current Detection System for the Combustion Limit Control", SAE paper 980171 (1998).
12. I. Andersson:
"Cylinder Pressure and Ionization Current Modeling for Spark Ignited Engines", Licentiate Thesis 2002
13. B. Johansson:
"Correlation Between Velocity Parameters Measured With Cycle-Resolved 2-D LDV and Early Combustion in a Spark Ignition Engine", ISRN LUTMDN/TMVK – 7012
14. S: Onishi, S. Hong Jo, K. Shoda, P Do Jo, S. Kato:
"Active Thermo-Atmosphere Combustion (ATAC) – A New Combustion Process for Internal Combustion Engines", SAE790501